MAUSAM, **76**, 3 (July 2025),733-744

MAUSAM

DOI : https://doi.org/10.54302/mausam.v76i3.6441
Homepage: https://mausamjournal.imd.gov.in/index.php/MAUSAM

UDC No. 551.553.21 : 551.577.37 (540.37)

Assessment of heavy rainfall cases during the monsoon 2022 over Arunachal Pradesh

A. SANDEEP[1*], ARUN VH[2#], S. I. LASKAR[3] and SUNIT DAS[2@]

[1]*Meteorological Centre Itanagar, India Meteorological Department, Arunachal Pradesh – 791 123, India*

[2]*Regional Meteorological Centre Guwahati, India Meteorological Department, Guwahati, Assam, India*

([#]arunkumar.vh@imd.gov.in, [@]sunit73.das@imd.gov.in)

[3]*India Meteorological Department, MoES, New Delhi, India* **(drsebul@gmail.com)**

(*Received 17 October 2023, Accepted 19 November 2024*)

***Corresponding author's email: drsandeepimd@yahoo.com**

सार – आईएमडी-ग्लोबल फोरकास्ट सिस्टम (GFS) मॉडल के पूर्वानुमानों के प्रदर्शन का मूल्यांकन अरुणाचल प्रदेश (ARP) के लिए 2022 के दक्षिण-पश्चिम मॉनसून के दौरान हुई वर्षा के आंकड़ों के आधार पर किया जाता है। 24 घंटों में ≥64.5 मिमी से अधिक वर्षा के कुल 14 मामलों की जांच की गई। प्रेक्षित और मॉडल दिन-1 की अनुमानित वर्षा के बीच 0.71 के सहसंबंध गुणांक (R) के साथ सहमती प्रदर्शित होती है, हालांकि, पूर्वानुमानित अग्रकाल बढ़ने के साथ R-मान 2-4% तक कम हो गए। इसके अतिरिक्त, पहले दिन के लिए मॉडल का प्रेक्षित वर्षा अनुमान 10-20% अधिक लगाया तथा अग्रकाल के बढ़ने के साथ इसमें 4-6% की और वृद्धि हुई। दिलचस्प बात यह है कि मॉडल पूर्वानुमानों ने 2022 के मॉनसून के दौरान अरुणाचल प्रदेश में 7-समांग HRF क्षेत्रों को दिखाया, जबकि प्रेक्षण ने केवल 5 क्षेत्रों को दिखाया। पूर्वानुमान प्रदर्शन का मूल्यांकन करने के लिए, प्रोबेबलिटी ऑफ डिटेक्शन (POD), फाल्स अलार्म रेट (FAR), एक्विटेबल थ्रेट स्कोर(ETS), और हेडके-कुइपर स्किल स्कोर (HK) जैसे कौशल मेट्रिक्स की गणना की गई। परिणाम दर्शाते हैं कि दिन-1 के पूर्वानुमानों के लिए POD 0.82 है और FAR 0.32 है जो HRF घटनाओं के सही पूर्वानुमान करने की उच्च दर को दर्शाता है। इसके अलावा, 0.43 का ETS और 0.38 का HK स्कोर मध्यम मॉडल प्रदर्शन दर्शाता है। अग्रकाल बढ़ने पर ये स्किल स्कोर 2-4% तक कम हो जाते हैं। इसके अलावा, मॉडल पूर्वानुमानों का मूल्यांकन चेतावनी रंग श्रेणी (पीले, नारंगी और लाल) के आधार पर किया जाता है। परिणाम उन दिनों के दौरान एक दिन के अग्रकाल पर क्रमशः सुझाव देते हैं, जब पीले रंग की चेतावनी दी जाती है, POD दर लगभग 0.80, जबकि नारंगी (लाल) चेतावनी के दिनों में POD दर 0.52 (0.25) होती है। यह दर्शाता है कि मॉडल पीले अलर्ट वाले दिनों में HRF घटनाओं का पूर्वानुमान करने में सबसे अच्छा प्रदर्शन करता है, लेकिन सभी अग्रकाल के लिए नारंगी और लाल अलर्ट वाले दिनों के लिए कम सटीक होता है।

ABSTRACT. The performance of IMD-Global Forecast System (GFS) model forecasts is evaluated against observed rainfall data during the southwest monsoon of 2022 for Arunachal Pradesh (ARP). A total of 14 heavy rainfall (HRF) cases were examined when the rainfall exceeds ≥64.5 mm in 24-hours. With a correlation coefficient (R) of 0.71 between the observed and model day-1 predicted rainfall exhibits a very good agreement, however, R -values were decreased by 2-4% as the forecast lead time increased. In addition, for day-1 model overestimated the observed rainfall by 10-20% and has increased further by 4-6% as the lead time progresses. Interestingly, the model forecasts noticed the 7-homogeneous HRF zones in ARP during the monsoon 2022, whereas the observations noticed only 5 zones. To assess forecast performance further, skill metrics such as Probability of Detection (POD), False Alarm Rate (FAR), Equitable Threat Score (ETS) and Heidke-Kuiper skill score (HK) were computed. Results show that the POD for day-1 forecasts is 0.82, and the FAR is 0.32 indicating a high rate of correctly predicting HRF events. In addition, ETS of 0.43 and HK score of 0.38 suggest moderate model performance. These skill scores decrease by 2-4% as lead time increases. Furthermore, the model forecasts are evaluated based on the warning color category (yellow, orange, and red). The results suggest during the days when the yellow alert is given the POD rate is about 0.80, whilst the orange (red) alert days the POD rate is 0.52 (0.25), respectively at one-day lead time. It indicates that the model performs is best in predicting HRF events during the yellow alert days but less accurate for orange, and red alert days for all lead times.

Key words – Heavy rainfall, Observational-data, IMD-GFS model forecasts, Impact-based forecast and Objective verification.

1. Introduction

The Indian Summer Monsoon (ISM) is a complex feedback system involving land-sea-atmosphere interactions with global connections, despite its regional meteorological dominance. In recent years, India has experienced an increase in heavy rainfall (HRF) events (rainfall > 64.5 mm in 24-hours) during the monsoon season exerts profound influence on agricultural production, water resources, and human lives. Thus, the accurate prediction of these events is very important and has major socioeconomic implications (Mahanta *et al.*, 2013; Wang *et al.*, 2015; Mohapatra *et al.*, 2021; Upadhyay *et al.*, 2023). North-East India (NEI) is hotspot for HRF occurrence (Pattanaik and Rajeevan, 2010) and associated flooding can cause severe damage. Many studies show an increasing trend in HRF occurrences across NEI during the monsoon season (Parthasarathy and Dhar, 1974; Sinha Ray and Srivastava, 2000; Goswami *et al.*, 2006; Subash *et al.*, 2010; Guhathakurta *et al.*, 2011; Mohapatra *et al.*, 2021). These HRF events are typically linked to large-scale synoptic systems such as low-pressure areas, active monsoon trough, mid-tropospheric circulation, and meso-scale circulations. (Rao, 1976; Webster, 1998; Goswami *et al.*, 2006; Mohapatra *et al.*, 2021). Additionally, orography also plays a vital role in the occurrence of HRF events over the study region (Mahanta *et al.*, 2013; Prokop and Walanus, 2015; Sharma *et al.*, 2019; Goswami *et al.*, 2010; Mohapatra *et al.*, 2008, 2021). Furthermore, Das *et al.* (2009) and (2015) showed that the distribution of heavy rainfall throughout the NEI during the SWM season is influenced by the location of the monsoon trough and synoptic systems like monsoon lows in and near NEI. Moreover, the spatial pattern of rainfall over NEI and the associated synoptic settings were studied in detail by Das Gupta (1967); Srinivasan, *et al.* (1972); Mohapatra *et al.* (2008) and (2011). Ramamurty (1969); Rao (1976); and Rahecha and Pisharoty (1996) concluded that the break monsoon conditions, when the monsoon trough is located near the foothills of the Himalayas, are very favorable for rainfall activity in NEI.

Numerical Weather Prediction (NWP) models have become an essential tool for routine weather forecasting, as well as for predicting the HRF events well in advance. Accurate prediction of HRF events is necessary as these events can lead to flash floods, landslides, soil erosion, & other disasters (IPCC, 2022). Several studies have examined the occurrence, trends, variability & verification of HRF events across India (Goswmai *et al.*, 2006; Rajeevan *et al.*, 2008; Mahanta *et al.*, 2013; Mohapatra *et al.*, 2009; Ashrit *et al.*, 2015; Satyanarayna & Kar, 2016; Sharma *et al.*, 2019; Mohapatra *et al*., 2021). Goswami *et al*., (2006) found an increasing trend in HRF events using IMD gridded rainfall data. Utilizing the same dataset, Rajeevan *et al.* (2008) highlighted the rising frequency of HRF events in central India. Satyanarayana and Kar (2016) also found similar results by using model forecasts. Mahanta *et al.* (2013) noticed that the most favorable period for HRF events in NEI is between 10 June & 5 Aug., whereas they have found a decreasing trend in HRF events. Sharma *et al.* (2019) noted an improvement in the model's ability to predict HRF events over NEI with skill scores increasing from 0.16 to 0.41 between 2007 & 2018. Further advancements were observed by Mohapatra *et al.* (2021) reported even more improvement in HRF forecast accuracy with skill scores rising by 48% during 2017-18, compared to 2002-16.

There hasn't been much research done on the verification of HRF occurrences over Arunachal Pradesh (ARP) (Khaladkar *et al*., 2009; Nandargi and Dhar, 2011; Bhagawati *et al*., 2018; Singh *et al*., 2021). Khaladkar *et al*. (2009) noticed that 23% of HRF events occurred at Passighat station in ARP during 1961-1980, with the frequency increased by 5% during 1981-2000. Bhagawati *et al.* (2018) found an increase in HRF events at Basar station in ARP from 1979 to 2015. Also, they found that the percentage contribution of HRF events to the annual total rainfall is higher compared to the light-to-moderate rainfall contribution. Singh *et al.* (2021) investigated the historical (1981 to 2019) and future (2021 to 2050) climate change situation using 15 extreme precipitation indices in Pare watershed of ARP. They found 12 indices showing decreasing trends during the historical period with statistically insignificant at the 95% confidence level, whilst 3 indices were found to be statically significant. In addition, they observed a decreasing trend at a rate of 3.13 mm per year during the historical period. In this paper, an effort has been made to assess the model forecast skill in respect to HRF events in ARP during the monsoon season of 2022.

The structure of the paper is organized as follows. Section 2 provides a detailed description of the study area, the data used, the synoptic situation, and the methodology adopted. Section-3 presents the results, focusing on the comparison between observed and model forecasted HRF events over ARP and summary statistics thereof. Special emphasis is given to the performance of model forecasts for different warning color categories at different lead times. Finally, the key results are summarized in Section 4.

2. Data and methodology

2.1. *Study area*

Arunachal Pradesh receives significant rainfall during the monsoon season (June to September) due to its location and topography, making it one of the wettest regions in NEI. The average rainfall of ARP is approximately 2800 mm (Bhagwati *et al.*, 2017; IMD 2022b) during the monsoon season. The eastern districts receive the highest rainfall often exceeding 4000 mm, whereas in western and central parts of ARP rainfall is approximately 25% lower than the eastern part.ARP is geographically located between 26.5 °N to 29.5 °N and 91.5 °E to 97.5 °E [Fig. 1(a)]. The terrain of ARP is predominantly mountains featuring the eastern Himalayas where elevations range from 60 m to 7000 m. The state's ecology features adiverse mix of dense forests, wetlands, and agricultural areas (mostly millets and fruits are grown). The state's climate is varied with subtropical conditions in the valley and alpine climate in higher altitudes. About 60% of annual total rainfall occurs between June and September, interestingly the contribution of heavy rainfall is approximately 45% (Sandeep *et al.* 2024). For the present study, the ARP region is divided into three zones, namely the western region (8 districts), the central region (8 districts) and the eastern region (9 districts).

2.2. *Description of observation data and model data*

The present study utilized two types of rainfall observations (*i*) IMD's high resolution 0.25° × 0.25° daily gridded rainfall data (Pai *et al.*, 2014) and (*ii*) station rainfall data. The first dataset is prepared by utilizing the daily rainfall data archived at the National Data Center in Pune. For the period 1979-2022, IMD has rainfall records from 6955 stations, among them IMD observatory stations (547), agromet stations (74), and the remaining stations are from state government offices. On average, rainfall data from 2600 stations per year were available for preparing the daily gridded dataset (Pai *et al.*, 2014). The second data was prepared by Meteorological Centre (MC) Itanagar using rainfall information from 56 stations collected from state government offices, and IMD observatory stations. All these stations are marked with the open red circles in Fig. 1(a). These rainfall datasets are augmented with the European Reanalysis version 5 (ERA-5) wind dataset that has a spatial resolution of 0.25 degrees latitude/longitude with a temporal resolution of 1-hour (Hersbach *et al.*, 2020).

This study also utilized the data from a high-resolution spectral model, *i.e.*, the Global Forecast System (GFS) run by IMD. This model provides medium-range forecasts with a horizontal resolution of T1534 (about ~12 km at mid-latitudes). This deterministic model has 64 sigma-pressure hybrid levels in the vertical. The dynamical core of the model is based on a semi-Lagrangian that has a spectral triangular truncation of

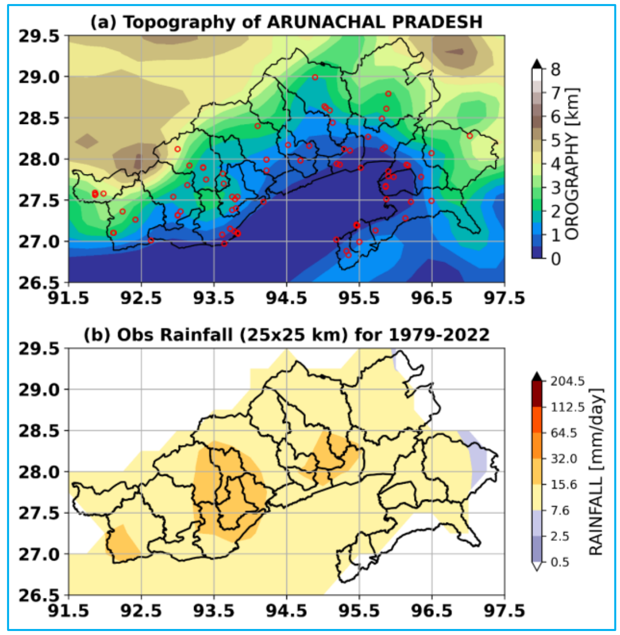

Figs. 1(a&b). (a) Topography of Arunachal Pradesh (study area) with rainfall recording stations marked with open red circles and (b) Climatological mean rainfall [mm/day] during the 1979 to 2022 period derived from IMD high-resolution daily gridded data

1534 waves. The model uses a four-dimensional variational data assimilation (4D-Var) scheme for generating initial conditions. The input data for this scheme is sourced from the global data assimilation system which is operational at NCMRWF (Prasad *et al.*, 2021). Global analysis was carried out four times per day (0000, 0006, 0012 and 0018 UTC) to produce the first guess, then the model produces global operational forecasts for 10 days twice a day, at 0000 UTC (0530 IST) and 0012 UTC (1730 IST). For this study, only day-1 to day-3 lead time forecasts were assessed. Further details about the operational configuration of the IMD-GFS model and parametrization schemes used can be found in IMD (2021).

2.3. *Synoptic situation of southwest monsoon 2022 over ARP*

During the ISM of 2022, the NEI region received an average of 713 mm rainfall, which is 82% of the long-period average of 870 mm, suggesting the below-normal monsoon. On the other side, APR experienced normal rainfall at 98% of its long-period average. The cumulative rainfall over ARP was 1430.3 mm against the normal rainfall of 1676.1 mm (departure is -15%) in the year 2022 (IMD, 2022b). The monsoon arrived in ARP on 3rd June, 2022, which was 2-day delay from the normal date, whilst the withdrawal of the monsoon was 15th October, 2022.

Considering the week-by-week rainfall analysis, out of 17-weeks (from 01 June, 2022 to 30 September, 2022) it has been found that 6-weeks were found to be have deficient rainfall (departure -59% to -19%), 4-weeks recorded normal rainfall (departure -19% to 19%), 3-weeks received excess rainfall (departure 20% to 59%), 2-weeks had large-excess rainfall (departure 60% or more), and 2-weeks had large deficient in rainfall (departure -99% to -60%) over ARP (IMD, 2022a). The long-term average of rainfall (1979 to 2022) during the monsoon season (June to September) over the study area is shown in Fig. 1(b). From this figure, climatologically the study area receives an average rainfall of ≥ 7.6 mm/day, indicates that moderate rain spells are very common in this region during the monsoon season.

The Impact Based Forecast (IBF) provides more actionable weather information by focusing on the consequences of severe weather (here it is for HRF event). IBF employs a risk matrix that calculates the warning level based on the severity and likelihood of an event's impact. The warnings are color-coded as follows: Green (no warning), Yellow (Watch), Orange (Be updated), and Red (Take action). Full details about the evaluation of the HRF warning system and IBF can be found in Mohapatra *et al.* (2021) and IMD (2021). MC Itanagar issued 14 IBF bulletins during the monsoon season 2022in association of HRF events in various districts of ARP. In totality, 164 districts were under yellow alerts, , orange and red alerts were issued for 46 and 2 districts, respectively(see the consolidated statement in Fig. 5). The number of yellow (orange) alerts is 153 (21) before 48-hours, and 106 (5) before 72-hours, respectively. All these IBF cases and their associated impacts are tabulated in Table 1. From this table, a total of 63 districts were impacted in ARP with almost 18,000 people affected by HRF events. A total of 26 people lost their lives and 36 land-slides were reported across the study area. In addition, 106 houses were damaged due to HRF and 108 cases of infrastructural damage (power lines, bridges, walls, road blockage, etc) were recorded. These impacts are collected from State Disaster Management Authority (SDMA) daily situation reports. During this study period, 121 districts were issued HRF warnings (7-11 cm in 24 hours), 55 districts issued very HRF warnings (12-20 cm in 24 hours), and 2 districts were alerted for extremely HRF warnings (>20 cm in 24 hours) in the study area. The total number of districts actually affected over the study area was 63, while the IMD-GFS model day-1 forecast issued warnings for 51 districts.

2.4. *Methodology*

To estimate the rainfall distribution (RFD) for those days when the HRF event is recorded for the study area, we have calculated the rainfall greater than 0.1 mm, and no rain days (*i.e.*, rainfall is equivalent to zero). The distribution of rainfall (percentage occurrence) is computed using Eqn. (1).

$$\mathrm{RFD} = 100x\,\frac{\text{Number of stations} \geq 0.1\text{mm}}{\text{Number of stations equivalent to } 0.0\text{mm} + \text{Number of ststions} \geq 0.1\text{mm}} \tag{1}$$

The computed RFD values were classified into five categories, namely dry (<1%), isolated (1%-25 %), scattered (26%-50%), fairly-widespread (51%-75%), and widespread (76%-100%). Hereafter they mentioned as DRY, ISOL, SCT, FWS and WS, respectively. The present study follows three rainfall intensity categories: HRF (64.5–115.5 mm in 24-hours), very HRF (115.6–204.4 mm in 24-hours), and extremely HRF (≥204.5 mm in 24-hours).

To evaluate the model's forecast performance, skill metrics were computed using a 2 × 2 contingency table, following Wilks (1995). The contingency table captures the correspondence between forecasted and observed rainfall events and categorizes outcomes into four groups, namely A (yes, yes): event forecasted and observed, B (yes, no): event forecasted but not observed, C (no, yes): event not forecasted but observed, and D (no, no): event neither forecasted nor observed. Based on this contingency table, the following statistical metrics were calculated to evaluate the model forecast performance.

Percentage Value = 100* [(model forecasted value – observed value)/(model forecasted value)]

$$\left.\begin{array}{ll}\text{Probability Of Detection (POD)} & = A/(A+B) \\ \text{False Alarm Rate (FAR)} & = C/(C+A) \\ \text{Equitable Threat Score (ETS)} & = A/(A+B+C)\end{array}\right\} \tag{2}$$

Heidke-Kuiper Skill Score (HK) = 2(AD-BC)/[(A+C)*(C+D) + (A+B)*(B+D)]

Percentage values are used for accounting the overestimation or underestimation of the model forecasts with respect to observations. POD measures the proportion of observed events that were correctly forecasted. FAR represents the proportion of forecasted

TABLE 1

Summary of IBF days when HRF event was realized in the study area and their corresponding impact

Date	Affected Districts/Village	Population Affected	Humans Lost	Land slides	Houses Damaged	Infrastructural damage
17.06.2022	Dibang Valley; Changlang; Lower Siang; West Kameng; Pakke Kessang; Upper Subansiri; Tawang	1039	1	3	5	9
18.06.2022	East Kameng; Leparada; West Kameng; Upper Subansiri; Tawang; Anjaw; Lohit; Pakke-Kessang; East Siang	63	1	2	5	7
19.06.2022	Kurung Kumey; Papum-Pare; Siang; Tawang; Lohit; West Kameng	74	1	4	7	9
28.06.2022	West Siang; Papum-Pare; East Siang; Siang; Namsai; Lower Dibang Valley; Lohit	7150	5	14	20	18
29.06.2022	Lower Subansiri; Upper Siang; Lower Siang; East Siang; Papum-Pare; Tirap; Lohit; Siang; West Kameng; Longding	1459	NIL	3	15	17
18.07.2022	Lohit; East Siang; Lower Dibang Valley; Upper Subansiri	2500	4	2	10	6
19.07.2022	Lohit; East Siang; Lower Dibang Valley; Lower Siang, Namsai	1500	2	1	8	4
31.07.2022	Papum-Pare; Siang; East Siang	850	NIL	1	4	2
01.08.2022	Siang; Lower Dibang Valley	600	3	1	7	9
27.08.2022	Siang; Lower Dibang Valley; Dibang Valley	1200	2	2	8	10
01.09.2022	Changlang	12	NIL	1	1	2
02.09.2022	Leparada	14	NIL	0	1	1
03.09.2022	Siang; Dibang Valley; Lower Dibang Valley; East Siang	1200	7	2	14	10
04.09.2022	Leparada; Lower Dibang Valley	8	NIL	0	1	4

events that did notoccur.ETS and HK metrics measure the overall accuracy and improvement of the forecast. For a perfect and accurate forecast; the ideal values of POD=1, FAR=0, and ETS=1. The HK score is a fractional improvement of the forecast over the standard observations, which is superior to other skill scores. HK ranges between -1 to +1 with 0 indicating no skill. These metrics provide valuable insights into the effectiveness and reliability of rainfall forecasts.

3. Results and discussion

In this section, the rainfall characteristics (spatial distribution and intensity) between observations and model forecasts at different lead times have been investigated first over the study area, and later over different cluster zones. Major concern is given to the performance of model forecasts for different color-coded warnings issued by IMD in the IBF system. The results from this analysis are expected to provide insights into the model's reliability for early warning systems, particularly in issuing timely and accurate alerts for HRF events.

3.1. *Characteristics of rainfall between observations and model forecasts*

Spatial variation of observed rainfall (combined gridded and station rainfall data) and model-predicted rainfall averaged for 14 days when HRF events occurred (as listed in Table 1) for different lead times is presented in Figs. 2(a-d). Observed rainfall in Fig. 2(a) is overlaid with mean wind vectors at the 700 hPa level from ERA-5 reanalysis outputs, while in Figs. 2(b-d) presented the model-predicted rainfalls with overlaid wind vectors at 850 hPa level from the IMD-GFS model forecasts for day-1, day-2, and day-3 lead times respectively. The winds show a southwesterly flow (a typical ISM circulation) and these winds carry moisture from the Bay of Bengal, contributing significantly to the occurrence of rainfall over the study area. Overall, the model forecasted winds also suggest similar circulation patterns. The interaction of these winds with the topography of ARP enhances the orographic lifting process, resulting in heavy rainfall. The mid-altitude regions (between 2-3 km) recorded the highest concentrations of HRF zones. Most

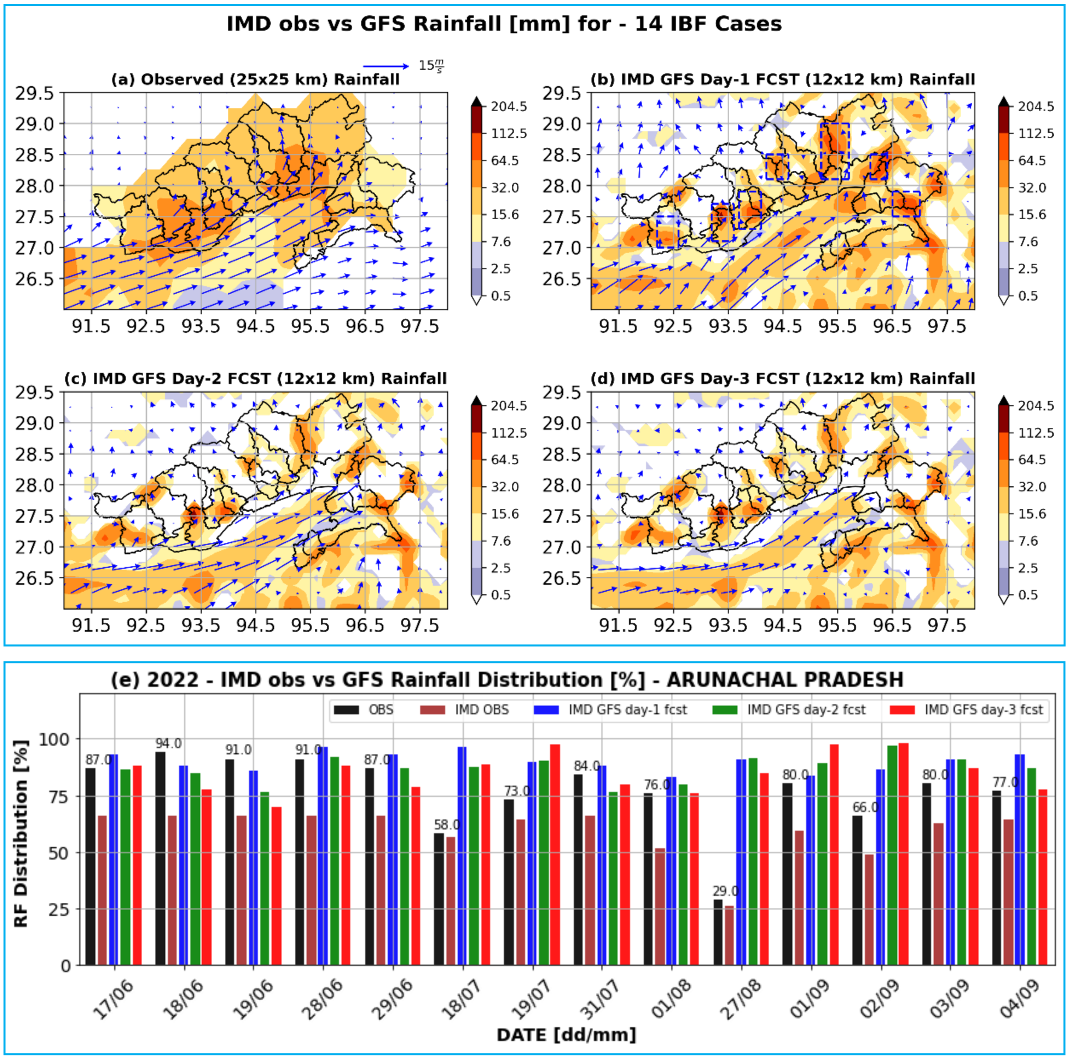

Figs. 2(a-e). Spatial distributions of (a) observed mean rainfall with overlaid mean wind vectors at 700 hPa level derived from ERA-5 reanalysis wind data. (b-d) Same as (a) but for IMD-GFS model forecasts at day-1, day-2, and day-3 lead times, respectively. The model rainfall data is overlaid with model forecasted winds at 850 hPa level. The blue color dashed boxes on (b) are the coherent zones [HRF zones]. (e) Case-to-case variation of rainfall distribution identified from station-level rainfall observations [black], daily gridded rainfall observations [brown], and model-predicted rainfall data for day-1, day-2, and day-3 lead times with blue, green, and red color bars, respectively

of this rainfall is primarily associated with the all India break monsoon conditions, and when the monsoon trough passes through or near the study area. The IMD-GFS model day-1 forecasts consistently over estimates the observed rainfall, and the error values (model minus observation) are slightly decreased for day-2 and day-3 lead times. On average, the observed rainfall over the study area was 24.7 mm, while the model predicted 29.2 mm rainfall for day-1, 26.08 mm rainfall for day-2, and 28.57 mm rainfall for day-3. Strikingly, the model forecasts identified 7- HRF zones (2 western, 3 central, and 2 eastern regions of ARP) which are marked in Fig. 1(b) with blue dotted boxes, whereas the observations registered only 3-HRF zones (one in each region). Overall, the IMD-GFS model exhibited approximately 10-20% higher amount of observed rainfall at one day lead time, and the model errors increased 4-6% per day for subsequent days.

The RFD occurrence percentage values were computed between observations (both gridded data and station level data) and model forecasts at 3-day lead times and the results are presented in Fig. 2(e). The black (brown) colour bars are realized RFD (percentage occurrences) computed from the station (gridded) rainfall data, whereas the blue, green, red colour bars are

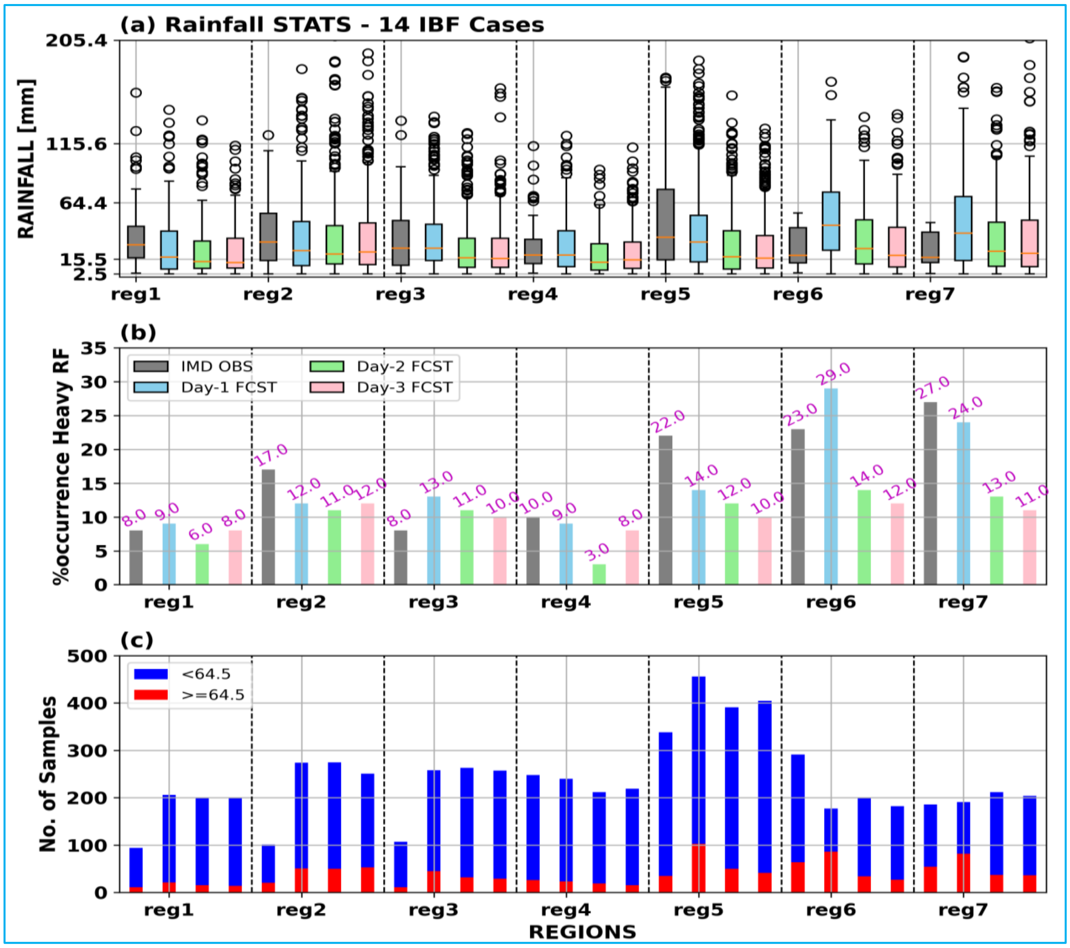

Figs. 3(a-c). (a) Area-averaged rainfall distributions in terms of boxplots forseven coherent zones identified in the study area between observations and model forecasts at different lead times. (b) Occurrence percentage of HRF events (>=64.4 mm to <115.5 mm in 24 hours) calculated between observations and model forecasts in different lead times. (c)Number of samples considered in each coherent zone for two different rainfall limits, with blue (red) indicatingthe rainfall less (greater) than 64.5 mm

computed from IMD-GFS model rainfall forecasts at day-1, day-2, day-3 lead-times, respectively. In most cases, the two types of rainfall observations show some variation in percentage occurrences, however despite their RFD class the average difference between the two is less than 5%. This indicates that local station-level rainfall data might capture small-scale variability more precisely. Out of 14 days, when HRF alerts were issued and realized, the station (gridded) rainfall data reported 10 (0) WS, 3 (13) FWS, and 1 (1) SCT, respectively, whereas the model day-1 forecast predicted all days with WS only. This suggests that the RFD category is relatively well predicted in the station rainfall observations. In totality, station level rainfall data corresponds well with the model forecasted rainfall (R=0.78), whilst the gridded rainfall observations have a slightly lower correspondence value (R=0.65) at one day lead time.

Furthermore, the rainfall verification was conducted over 7 cluster-zones identified by the model (2 in the western, 3 in the central, and 2 in the eastern regions of ARP) based on the spatial distribution and the comparison results are presented in Fig. 3. Fig. 3(a) presents the rainfall distributions in terms of boxplots between the observations (combined both the gridded and station level rainfall data) and the model forecasted rainfall at different lead times, where the box comprises 50% of data, and the top and bottom whiskers comprise 5% and 95%, respectively. From the figure, it is clear that the model forecasts identified 7-HRF zones at all lead times, but only 5 regions realized HRF events in the observations. In addition, two regions (regions 2 and 5) forecasted the extremely HRF events (>204 mm in 24 hours), but only one region (region 2) is seen in the observations. The model showed a tendency to over estimate rainfall in the

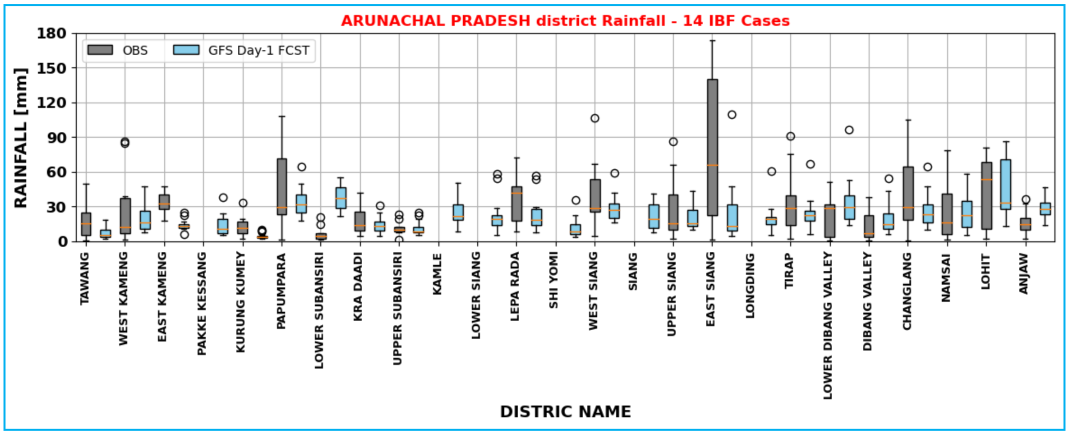

Fig. 4. Distributions (in terms of boxplot) of rainfall in each district of the study area between observations and model day-1 forecasts. All 14 HRF cases are considered for this distribution, where the box comprises 50% of values (25^{th} and 75^{th} percentiles) and whiskers represent 5thand 95^{th} percentile values

ARUNACHAL PRADESH District wise Weather Warnings

District	17062022	18062022	19062022	28062022	29062022	18072022	19072022	31072022	01082022	27082022	01092022	02092022	03092022	04092022
WESTERN ARUNACHAL PRADESH														
	Day1	Day1	Day1	Day1	Day1	Day1	Day1	Day1	Day1	Day1	Day1	Day1	Day1	Day1
TAWANG	No Wx	No Wx	No Wx	No Wx	No Wx	No Wx	TSL	TSL	No Wx	TSL	No Wx	No Wx	No Wx	No Wx
WEST KAMENG	EHRF	VHRF	VHRF	HRF	No Wx	TSL	TSL+VHRF	TSL+HRF	TSL+HRF	No Wx	TSL+HRF	No Wx	No Wx	TSL+HRF
EAST KAMENG	VHRF	HRF	HRF	HRF	No Wx	TSL+HRF	TSL+HRF	TSL+HRF	TSL+HRF	TSL+HRF	TSL+HRF	TSL+HRF	TSL	TSL+HRF
KURUNG KUMEY	No Wx	No Wx	No Wx	No Wx	No Wx	TSL	No Wx	TSL+HRF	No Wx	TSL	TSL+HRF	No Wx	TSL+HRF	No Wx
KRA DAADI	VHRF	HRF	No Wx	HRF	No Wx	No Wx	HRF	HRF	No Wx	No Wx	No Wx	TSL+HRF	TSL	No Wx
UPPER SUBANSIRI	No Wx	No Wx	No Wx	HRF	No Wx	TSL	No Wx	TSL+HRF	TSL+HRF	TSL+HRF	TSL+HRF	No Wx	No Wx	TSL+HRF
LOWER SUBANSIRI	VHRF	VHRF	VHRF	HRF	VHRF	TSL	TSL+HRF	TSL+HRF	TSL+HRF	TSL+HRF	TSL+HRF	No Wx	TSL+HRF	TSL+HRF
PAKKE KESSANG	VHRF	HRF	No Wx	HRF	HRF	TSL+HRF	TSL+HRF	TSL+HRF	TSL+HRF	TSL+HRF	No Wx	TSL+HRF	TSL+HRF	TSL+HRF
PAPUMPARE	VHRF	HRF	No Wx	HRF	HRF	TSL+HRF	TSL+HRF	TSL+VHRF	TSL+HRF	TSL+HRF	No Wx	TSL+HRF	TSL+HRF	TSL+HRF
CENTRAL ARUNACHAL PRADESH														
WEST SIANG	No Wx	No Wx	HRF	HRF	No Wx	TSL+HRF	TSL	TSL+HRF	No Wx	No Wx	TSL+HRF	No Wx	TSL+HRF	TSL+HRF
SIANG	VHRF	No Wx	HRF	EHRF	HRF	TSL+VHRF	HRF	VHRF	VHRF	TSL+HRF	HRF	TSL+HRF	TSL+VHRF	TSL+VHRF
KAMLE	No Wx	No Wx	No Wx	No Wx	No Wx	No Wx	No Wx	No Wx	No Wx	No Wx	HRF	No Wx	No Wx	No Wx
SHIYOMI	No Wx	No Wx	No Wx	No Wx	No Wx	No Wx	No Wx	No Wx	No Wx	No Wx	No Wx	No Wx	No Wx	No Wx
LEPA RADA	No Wx	No Wx	No Wx	HRF	HRF	TSL	HRF	HRF	No Wx	No Wx	No Wx	TSL+HRF	No Wx	TSL+HRF
UPPER SIANG	No Wx	No Wx	No Wx	VHRF	No Wx	TSL	HRF	HRF	HRF	TSL+HRF	TSL+HRF	TSL+HRF	TSL+VHRF	TSL+VHRF
EAST SIANG	HRF	HRF	HRF	EHRF	HRF	TSL+VHRF	TSL+HRF	TSL+VHRF	TSL+HRF	TSL+HVHRF	No Wx	TSL+HRF	TSl+HRF	TSL+EHRF
LOWER SIANG	No Wx	HRF	HRF	HRF	No Wx	TSL+VHRF	TSL+VHRF	HRF	No Wx	TSL+HRF	TSL+HRF	TSL+HRF	TSL+HRF	TSL
EASTERN ARUNACHAL PRADESH														
LOWER DIBANG VALLEY	VHRF	HRF	HRF	VHRF	HRF	TSL+VHRF	TSL+VHRF	No Wx	TSL+VHRF	TSL+VHRF	No Wx	TSL	TSL+HRF	TSL+VHRF
DIBANG VALLEY	HRF	VHRF	HRF	HRF	No Wx	TSL+HRF	TSL+HRF	TSL	TSL+HRF	TSL+VHRF	TSL+HRF	TSL	TSL+VHRF	TSL+VHRF
ANJAW	VHRF	VHRF	No Wx	No Wx	VHRF	TSL	No Wx	TSL	TSL	TSL	HRF	No Wx	No Wx	TSL+HRF
LOHIT	VHRF	HRF	HRF	VHRF	VHRF	TSL+VHRF	TSL+VHRF	TSL	TSL	TSL+VHRF	No Wx	No Wx	TSL	TSL+VHRF
NAMSAI	HRF	VHRF	No Wx	HRF	VHRF	TSL+VHRF	TSL+VHRF	No Wx	No Wx	TSL+VHRF	TSL	TSL+HRF	No Wx	TSL+HRF
CHANGLANG	No Wx	vHRF	No Wx	HRF	HRF	TSL+HRF	TSL+HRF	No Wx	No Wx	TSL+HRF	No Wx	TSL	TSL	TSL
TIRAP	No Wx	HRF	No Wx	HRF	HRF	No Wx	TSL+HRF	TSL	TSL	TSL+HRF	TSL	No Wx	No Wx	TSL
LONGDING	HRF	HRF	No Wx	No Wx	HRF	TSL	No Wx	No Wx	No Wx	TSL	No Wx	No Wx	No Wx	No Wx

Fig. 5. Impact Based Forecasts issued for each district in the study area during the southwest monsoon 2022. The district name (date) is provided on the left (upper) side. Each colour coded category indicates the warning level. A total of 164 yellow alerts, 46 orange alerts, and 2 red alerts were issued at the district level before 24 hours. Here HRF: Heavy Rainfall, VHRF: Very Heavy Rainfall, EHRF: Extremely Heavy Rainfall

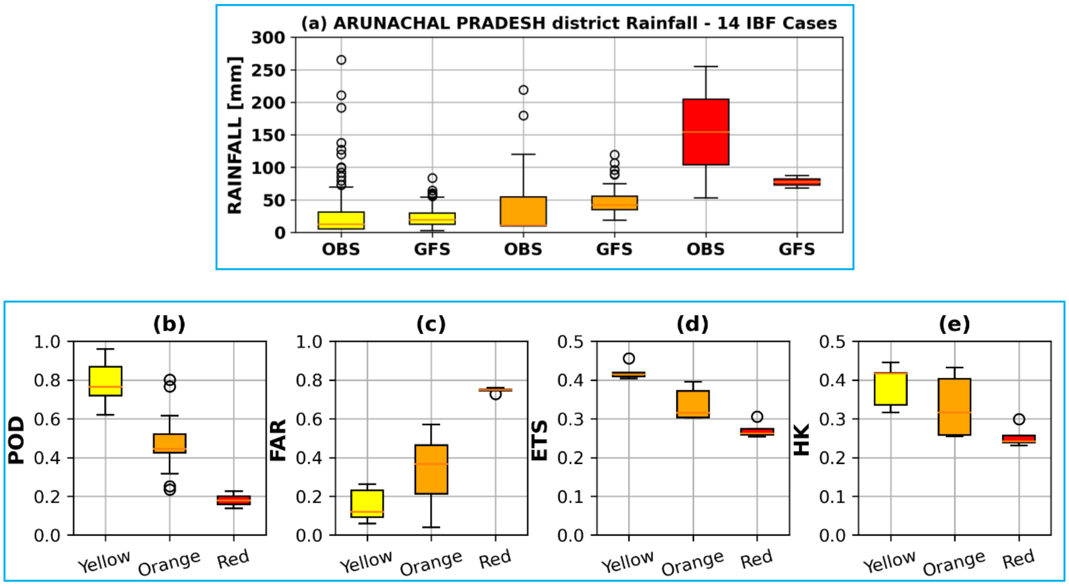

Figs. 6(a-e). (a) Rainfall Distributions for observations and model day-1 forecasts as function of warning category. Distributions of statistical metrics computed between observations and model day-1 forecasts such as (b) Probability of Detection, (c) False Alarm Rate, (d) Equitable Threat Score, and (e) Heidke-Kuiper Skill Score as a function of the warning category. These distributions are shown as box plots, where the box comprises 50% of values (25^{th} and 75^{th} percentiles) and whiskers represent 5^{th} and 95^{th} percentile values

western and central regions of ARP and while to underestimate it in the eastern region. In Fig. 3(b), the occurrence percentage of HRF against available observations is presented bar plot at different lead times. The number of samples utilized for obtaining the percentage values is given in Fig. 3(c), where blue (red) colors represent the samples considered for below (above) 64.5 mm. On average, the three regions of study are such as western, central, and eastern ARP realized 12%, 13%, and 25% of HRF occurrence, whilst the model slightly under(over) estimates the occurrence in the western and central (eastern) regions with approximately 1-2% difference at one day lead time. Additionally, the difference between the model minus realized HRF occurrence increased to ~40% at day-2 and day-3 lead times. Overall, the model's day-1 forecast had a ~90% match with the actual HRF occurrence across all regions. The region 7 exhibited higher frequency of HRF and the region1 recorded lower frequency in both observations and forecasts. The eastern side of ARP appears more prone to HRF events in 2022, while the western side of ARP is less prone.This detailed verification suggests that rainfall patterns were well captured by the model on day-1 forecasts but became less accurate as lead time increased, particularly in HRF-prone zones in eastern ARP.

The district-level analysis of ARP highlights some important observations regarding the model's performance in predicting rainfall, particularly for HRF events in the year 2022. Fig. 4 presents the distributions of rainfall in terms of box plots between observations and model day-1 forecasts for 25 districts in ARP. Two interesting points are inferred from here. (*i*) Most of the districts have noticed wider rainfall distributions (approximately 60%) in the observations, whereas the model day-1 forecasts are relatively less wider. (*ii*) The observed average rainfall amountsat East Siang and Lohit districts are 60.5 mm and 55.2 mm indicating the most prominent districts for HRF occurrence, whereas the model predicted the rainfall is 30.2 mm and 44.5 mm. Observations recorded 37 stations with HRF events, while the model forecasted 105 HRF stations. For very HRF eventsthe observations reported 17 stations but the model predicted54 stations, whereas for extremely HRF events only 4 stations were observed, but the model forecasted just 2 at one day lead time. The model'serror in forecasting HRF events was 36% for HRF, 31% for very HRF, and 50% for extremely HRF. These errors grow 4-6% per day. On 28^{th} June 2022,the model successfully predicted the realized HRF event at two stations in the East Siang districtfor all lead times. Moreover, on two dates (17 June and 4 Septemeber) the model failed to predict extreme HRF event before 48 and 72 hours though it is realized in the observations and mode day-1 forecast.

3.2. *Performance of model forecasts as a function of weather warning*

In 2022, MC Itanagar issued 14 IBF bulletins at the district level to alert the HRF events well in advance. The

TABLE 2

The average values of statistical metrics computed between observations and model forecasts for yellow, and orange alert categories when the HRF event was issued in the study area. The total number of samples for the yellow alert at day-1, day-2, and day-3 lead times are 2348, 2190 and 1517, respectively, while for orange alerts the sample sizes are 439, 200 and 50

Observations *vs* Forecasts	Day-1	Day-2	Day-3
Yellow alert [2348, 2190, 1517]			
POD	0.83	0.81	0.78
FAR	0.17	0.22	0.22
ETS	0.44	0.43	0.42
HK	0.38	0.39	0.38
Orange alert [439, 200, 50]			
POD	0.55	0.53	0.50
FAR	0.45	0.37	0.50
ETS	0.35	0.34	0.34
HK	0.35	0.36	0.35

consolidated IBF statement for these 14 HRF cases is shown in Fig. 5. A comparison of rainfall data between observations and model day-1 forecast is presented in Fig. 6(a) for different color codes. Interesting inferences are drawn from here. (*i*) During yellow and orange alert times, the model over-predicted the realized rainfall, whereas during the red alert time rainfall is under-predicted. (*ii*) The occurrence percentages of HRF events during the yellow, orange, and red alerts issued are 32%, 18%, and 52%, respectively. Nevertheless, the model forecasts slightly overestimated these values with errors increasing according to the severity of the color-coded warning.

Furthermore, skill metrics were computed using Eqn. (2) to evaluate the model performance for each color-coded warning category (yellow, orange, and red) in forecasting rainfall. The skill metrics such as POD, FAR, ETS and HK between observed rainfall and model forecasted rainfall at one day lead time are shown in terms of box plots in Figs. 6(b-e), where the box comprises 50%of values. The mean values of these metrics are summarized in Table 2 for alllead times. As seen in Fig. 6(b), POD values are in the range of 0.6 to 0.9 (on average 0.80) for 2022 when the yellow warning is issued, indicating model performance is very good. However, for orange warnings the average POD is 0.51suggesting the model performance is moderate. POD values are less than 0.25 when red warnings are issued signaling poor model performance for HRF events. FAR values also suggesting the similar results that during the yellow warning time model day-1 forecast missed the less HRF events, whilst during the red warning the missing HRF events were more. ETS values showed less variability, implying the model day-1 forecast performance remained relatively stable across different warnings. HK values suggested that the model performance is above 50% for all color-coded warnings. Overall, the model performs well in predicting the HRF events at day-1 lead time, but its effectiveness in predicting the number of affected districts decreases with longer lead times.

4. Conclusions

In recent times, HRF events have become more frequent, leading to flash floods, triggering landslides and causing significant damage to property, infrastructure and loss of lives in ARP. IBF alerts have been issued 24 to 72 hours ahead to minimize the impacts of these HRF events. This paper analyzes the 14 IBF cases during the 2022 monsoon season in Arunachal Pradesh, with a special focus on HRF alerts, examining how model forecasts predicted these events at different lead times and during different color-coded warning times. The following broad conclusions are drawn:

(*i*) The IMD GFS model approximately 10-20% over predicted the observed rainfall at all lead times, with error values increasing by 5-6% per day. A very good correspondence is seen between observed and model day-1 forecasted rainfall, registering the correlation coefficient (R) of 0.71, however, R -values were decreased by 2-4% as the forecast lead time increased. Additionally, the station rainfall data corresponds well with the model-predicted day-1 rainfall achieving an R-value of 0.78.Out of 14 days, when HRF alerts were issued and realized, the station (gridded) rainfall data reported 10 (0) WS, 3 (13) FWS, and 1 (1) SCT, respectively, whereas the model day-1 forecast predicted all days with WS only. This suggests that the RFD category is relatively well predicted in the station rainfall observations.

(*ii*) The model forecasts identified 7 significant HRF zones at all lead times, but observations only confirmed HRF events in 5 regions. In particular, two regions (regions 2 and 5) were forecasted to experience extremely HRF events (>204 mm in 24 hours), but only one region (region 2) is realized in the observations. On average, the western, central, and eastern ARP regions realized 12%, 13%, and 25% of HRF occurrence, respectively. The model slightly underestimated HRF in the western and central regions and overestimated it in the eastern region with approximately 1-2% difference at one day lead time. Overall, there is ~90% match between the model day-1 forecast and realized HRF occurrence.

(*iii*) During the yellow and orange alert times, the model over predicted the realized rainfall, whereas during the red alert time, it is under predicted the rainfall. The occurrence percentage of HRF events during yellow, orange and red alert times was 32%, 18% and 52%, respectively. The model forecasts slightly over estimated these percentage values during the yellow alert time and during the orange and red alert times the error values increased approximately 6-8%. The POD value is found to be higher for the yellow warning (0.80), followed by the orange warning (0.51) and was statistically insignificant for the red warning. The FAR values are increased as a function of color-coded warnings. Both the POD and FAR values suggest that during the yellow alert time the model performance is very good, whereas during the orange alert time model performance is moderate & during the red alert time model performance is poor in predicting the HRF events. ETS values showed less variability, implying that model day-1 forecast accuracy remained relatively stable across different warnings. HK values suggested that model performance was above 50% across all color-coded categories.

Despite the accurate and timely issuance of IBF alerts, weather-related hazards continue to cause significant loss of lives, damage to property and infrastructure. The IMD plays pivotal role in making critical decisions to minimize the damage from such events. In light of this, to enhance disaster preparedness, the risk matrix needs to be updated and improved further with the collaboration of other agencies. Enhancing the four-stage IBF process, from hazard likelihood assessment to evaluating potential impacts, will be crucial in future studies for better mitigation and preparedness against extreme weather events.

Acknowledgements

The authors would like to thank the NWP division, IMD for providing the valuable IMD-GFS model forecasts and gridded rainfall data and the State Disaster Management Authority, Arunachal Pradesh for supplying the daily situation reports. Special thanks to the Director General of Meteorology, IMD M. Mohapatra and the Head, RMC Guwahati K. N. Mohan for providing the necessary facilities to carry out this work.

Authors' Contributions

A. Sandeep: Conceptualization, Methodology, Software, Validation, Analysis, Investigation, Resources, Data Collection, Draft Preparation And Editing, Visualization, Project Administration, Resources.
Arun VH: Methodology, Analysis, Resources, Writing-Review And Editing, Visualization.
S. I. Laskar: Resources, Data Collection, Supervision.
Sunit Das: Validation, Investigation, Data Collection, Supervision, Project Administration.

Data Availability: The datasets generated during and/or analysed during the current study are available from the India Meteorological Department upon reasonable request.

Conflict of Interest: The authors declare no competing interests.

Disclaimer: The contents and views presented in this research article/paper are the views of the authors and do not necessarily reflect the views of the organizations they belongs to.

References

Ashrit, R., Sharma, K., Dube, A., Iyengar, G., Mitra, A. and Rajagopal, E. N., 2015, "Verification of short range forecasts of extreme rainfall during monsoon", *MAUSAM*, **66**, 375-386. doi: https://doi.org/10.54302/mausam.v66i3.548.

Bhagawati, K., Sen, A., Kalita, H., Bhagawati, R. and Shukla, K. K., 2018, "Rainy days and rainfall intensity trends in Basar (Arunachal Pradesh) during 1979-2015", *MAUSAM*, **69**, 3, 427-432. https://doi.org/10.54302/mausam.v69i3.333.

Das Gupta, D. N., 1967, "Study of heavy rainfall associated with low pressure micro-cells over Northeast India", *Indian J. Met. & Geophys.*, **18**, 101-104. https://doi.org/10.54302/mausam.v18i1.4004.

Das, S., Bhattacharjee, K., Ali, P., Luitel, M., Choudhury, A., Shaw, S. O. and Hazarika, G., 2015, "Quantitative precipitation forecast for the Brahmaputra and the Barak basins by synoptic analogue technique", *MAUSAM*, **66**, 1, 43-76. https://doi.org/10.54302/mausam.v66i1.367.

Das, S., Mohapatra, M. and Ram, S., 2009, "Some characteristics of heavy rainfall events over Northeastern states of India", *MAUSAM*, **60**, 4, 525-533. https://doi.org/10.54302/mausam.v60i4.1120.

Goswami, B. B., Mukhopadhyay, P., Mahanta, R. and Goswami, B. N., 2010, "Multiscale interaction with topography and extreme rainfall events in the northeast Indian region", *J. Geophys. Res*. (Atmosphere), **115**, D12114, doi:10.1029/2009jd012275.

Goswami, B. N., Venugopal, V., Sangupta, D., Madhusoodanan, M. S. and Xavier, P. K., 2006, "Increasing trend of extreme rain events over India in a warming environment", *Science*, **314**, 5804, 1442-1445. https://doi.org/10.1126/science.1132027.

Guhathakurta, P., Sreejith, O. P. and Menon, P. A., 2011, "Impact of climate change on extreme rainfall events and flood risk in India", *J. Earth Syst. Sci*., **120**, 359-373. https://doi.org/10.1007/s12040-011-0082-5.

Hersbach, H., Bell, B., Berrisford, P., Hirahara, S., Horányi, A., Muñoz-Sabater, J., Nicolas, J., Peubey, C., Radu, R., Schepers, D., Simmons, A., Soci, C., Abdalla, S., Abellan, X., Balsamo, G., Bechtold, P., Biavati, G., Bidlot, J., Bonavita, M., … Thépaut, J. N., 2020, "The ERA5 global reanalysis", *Quarterly Journal of the Royal Meteorological Society*, **146**, 730, 1999-2049. https://doi.org/10.1002/qj.3803.

IMD, 2021, "Standard operation procedure – Weather Forecasting and Warning Services", 1-331. https://mausam.imd.gov.in/imd_latest/contents/pdf/forecasting_sop.pdf.

IMD, 2022a, "Annual report of 2022", 1-169, https://mausam.imd.gov.in/imd_latest/contents/ar2022.pdf.

IMD, 2022b, "Rainfall statistics of India 2022", 1-21, https://hydro.imd.gov.in/hydrometweb/(S(4hkzgw45qtw3od551duscx55))/PR

ODUCTS/Publications/Rainfall%20Statistics%20of%20India%20-%202022/Rainfall%20Statistics%20of%20India%202022.pdf.

IPCC, 2022, "Climate Change 2022 : Mitigation of Climate Change, working group III contribution to the sixth assessment report of the Intergovernmental panel on climate change", 1-2029, https://www.ipcc.ch/report/sixth-assessment-report-working-group-3/.

Khaladkar, R., Mahajan, P. and Kulkarni, J., 2009, "Alarming Rise in the Number and Intensity of Extreme Point Rainfall Events over the Indian Region under Climate Change Scenario", *Indian Institute of Tropical Meteorology*, https://www.tropmet.res.in/~lip/Publication/RR-pdf/RR-123.pdf.

Mahanta, R., Sarma, D. and Choudhury, A., 2013, "Heavy rainfall occurrences in northeast India", *International Journal of Climatology*, **33**, 6, 1456-1469. https://doi.org/10.1002/joc.3526.

Mohapatra, M., Biswas, H. R. and Sawaisarje, G. K., 2011, "Spatial variability of daily rainfall over Northeast India during summer monsoon season", *MAUSAM*, **62**, 2, 215-228. doi : https://doi.org/10.54302/mausam.v62i2.288.

Mohapatra, M., Biswas, H. R. and Swaisarje, G. K., 2008, "Daily summer rainfall over northeast India due to synoptic scale systems", *MAUSAM*, **59**, 35-50. https://doi.org/10.54302/mausam.v59i1.1130.

Mohapatra, M., Hatwar, H. R., Bandyopadhyay, B. K. and Subrahmanyam, V., 2009, "Evaluation of heavy rainfall warning over India during summer monsoon season", *MAUSAM*, **60**, 4, 475-490. https://doi.org/10.54302/mausam.v60i4.1116.

Mohapatra, M., Kumar, N., Mishra, K. and Devi, S., 2021, "Evaluation of heavy rainfall warnings of India National Weather Forecasting Service for monsoon season (2002-2018)", *Journal of Earth System Science*, **130**, 1. https://doi.org/10.1007/s12040-020-01549-z.

Nandargi, S. and Dhar, O. N., 2011, "Extreme rainfall events over the Himalayas between 1871 and 2007", *In Hydrological Sciences Journal*, **56**, 6, 930-945). https://doi.org/10.1080/02626667.2011.595373.

Pai, D. S., Sridhar, L., Rajeevan, M., Sreejith, O. P., Satbhai, N. S. and Mukhopadyay, B., 2014, "Development of a new high spatial resolution (0.25° × 0.25°) Long Period (1901-2010) daily gridded rainfall data set over India and its comparison with existing data sets over the region", *MAUSAM*, **65**, 1. doi: https://doi.org/10.54302/mausam.v65i1.851.

Parthasarathy, B. and Dhar, O. N., 1974, "Secular variations of regional rainfall over India", *Quarterly Journal of the Royal Meteorological Society*, **100**, 424, 245-257. https://doi.org/10.1002/qj.49710042411.

Pattanaik, D. R. and Rajeevan, M., 2010, "Variability of extreme rainfall events over India during southwest monsoon season", *Meteorological Applications*, **17**, 1, 88-104. https://doi.org/10.1002/met.164.

Prokop, P. and Walanus, A., 2015, "Variation in the orographic extreme rain events over the Meghalaya Hills in northeast India in the two halves of the twentieth century", *Theoretical and Applied Climatology*, **121**, 1-2, 389-399. https://doi.org/10.1007/s00704-014-1224-x.

Rahecha, P. R. and. Pisharoty, P. R., 1996, "Heavy rainfall during monsoon season : Point and spatial distribution", *Current Science*, **71**, 3, 179-186.

Rajeevan, M., Bhate, J. and Jaswal, A. K., 2008, "Analysis of variability and trends of extreme rainfall events over India using 104 years of gridded daily rainfall data", *Geophysical Research Letters*, **35**, 18. https://doi.org/10.1029/2008GL035143.

Ramamurthy, K., 1969, "Monsoon of India: some aspects of the 'break' in the Indian southwest monsoon during July and August", *Forecasting Mannual*, 18.3 (No. IV) : 1 - 57, India Meteorological Department, Pune, https://www.imdpune.gov.in/Reports/Forecasting_Mannuals/IMD_IV-18.3.pdf.

Rao, Y. P., 1976, "Southwest monsoon : Synoptic meteorology", Meteor. Monogr., No. 1/1976, India Meteorological Department, https://imetsociety.org/wp-content/pdf/docs/swmonsoon_yprao.pdf.

Rao, Y. P., 1976, "Southwest Monsoon", Meteorological Monograph Synoptic Meteorology No. 1/1976, India Meteorological Department, Pune, p367, https://imetsociety.org/wp-content/pdf/docs/swmonsoon_yprao.pdf.

Sandeep, A., Das, S. and Aru, V. H., 2024, "An observational study on the variability and climatology of Arunachal Pradesh", *Pure. Appl. Geophys.*, (under revision).

Satyanarayana, G. C. and Kar, S. C., 2016, "Medium-range forecasts of extreme rainfall events during the Indian summer monsoon", *Meteorological Applications*, **23**, 2, 282-293. https://doi.org/10.1002/met.1553.

Sharma, K., Kumar, S., Ashrit, R., Milton, S., Mitra, A. K. and Rajagopal, E. N., 2019, "Evaluation of Unified Model Rainfall Forecasts over the Western Ghats and North East states of India", *Geo. Sci. Mod. Dev*., https://doi.org/10.5194/gmd-2019-65

Singh, W. R., Barman, S., Sharma, S. K., Taggu, A., Bandyopadhyay, A. and Bhadra, A., 2021, "Historical and projected precipitation extremes over Pare watershed in Arunachal Pradesh, India", *Applied Water Science*, **11**, 3. https://doi.org/10.1007/s13201-021-01382-9.

Sinha Ray, K. C. and Srivastava, A. K., 2000, "Is there any change in extreme events like heavy rainfall?", *Current Science*, **79**, 2, 155-158.

Srinivasan, V., Raman, S. and Mukherjee, S., 1972, "Southwest Monsoon - Typical situation over West Bengal, Assam and adjoining States", IMD, FMU Rep. III 3.6.

Subash, N., Sikka, A. K. and Mohan, H. S. R., 2010, "An investigation into observational characteristics of rainfall and temperature in Central Northeast India-a historical perspective 1889-2008", *Theoretical and Applied Climatology*, **103**, 3-4, 305-319. https://doi.org/10.1007/s00704-010-0299-2.

Upadhyay, H., Singh, P. K. and Kothar, M., 2023, "Climate Change and Consequential Rainfall Trends : An Indian Perspective", *Ecology, Environment and Conservation*, **29**, S124–S131. https://doi.org/10.53550/eec.2023.v29i01s.019.

Wang, B., Xiang, B., Li, J., Webster, P. J., Rajeevan, M. N., Liu, J. and JaHa, K., 2015, "Rethinking Indian monsoon rainfall prediction in the context of recent global warming", *Nature Comm*., **6**, 7154. doi: 10.1038/ncomms8154.

Webster, P. J., Magana, V. O., Palmer, T. N., Shukla, J., Tomas, R. T., Yanai, M. and Yasunari, T., 1998, "Monsoons : processes, predictability and the prospects of prediction", *J. Geophys. Res*., **103**, 14451-14510. doi: 10.1029/97JC02719.

Wilks, D.S., 1995, Statistical Methods in the Atmospheric Sciences, Academic Press, San Diego, 467 p. https://sunandclimate.wordpress.com/wp-content/uploads/2009/05/statistical-methods-in-the-atmospheric-sciences-0127519661.pdf.